50th AIAA Aerospace Sciences Meeting and Exhibition
9-12 January 2012, Nashville, TN, USA

AIAA 2012-0662

Discharge processes in a stratosphere and mesosphere during a thunder-storm

Kirill V. Khodataev*
Moscow Radiotechnical Institute RAS, Russia

k.v.k@home ptt.ru

The work is devoted to the further theory development of the discharge phenomena called elves and sprites in a stratosphere and mesosphere initiated by tropospheric storm processes. At a quantitative level the process of redistribution of charges in an atmosphere at altitudes up to 150 km during charging and discharging of a storm cloud is investigated. An important role of the small electric conductivity of the stratosphere and mesosphere is shown. At lightning discharge of a storm cloud the area of the overcritical field appears under the ionosphere in which the avalanche ionization arises (elf). The avalanche ionization front instability causes the growth of large-scale perturbances developing into an area of a subcritical field and initiating the system of subcritical streamer discharges. The account of the small electric conductivity of the atmosphere between the troposphere and the ionosphere has allowed to explain the long duration of discharge processes developing under the ionosphere, basically, in the residual electrostatic polarization field.

Keywords: plasma, ionosphere, mesosphere, discharge, streamer, elves, sprites, ionization avalanche, thunderstorm, clouds, lightning.

1. Introduction

Pioneer visual observations of the high-altitude discharges from planes and orbital stations in 89-91 years of the last century[1,2] have stimulated regular scientific researches of an unknown phenomenon[3,4,5,6,7] devoted to accumulation of experimental data. The stream of the publications devoted to the further studying of phenomenology, experimental and theoretical research of high-altitude discharges in increasing rate proceeds by this day. The review of works on this topic can be found in many references, in particular, in Ref.[8,9].

By present time a large volume of discharge processes observations in the stratosphere and mesosphere is collected and a construction of the self-consistent closed theory of these phenomena is continued by a wide front.

Among high-altitude discharges one can distinguish the ascending (blue jets) and the descending discharges (sprites). Present article is devoted to constructing of a quantitative theory of the descending discharges of elves and sprites type.

Shortly the data of descending discharges observations are reduced to the following.

On the night side of the Earth above the horizon on a background of the dark sky luminescence flashes at altitude about 90 km with a radius of a luminous disk ~100 km are observed from time to time. Duration of the flashes is of

* Investigator, Dr. Sci., professor, member AIAA

order 0.1÷1 ms. In Fig. **1** one of the first photos of such flashes made from the earth surface made in America in 1997, Ref.[10], (see Fig. **1a**) and from a board of the shuttle Columbia (January, 19 2003) at night above the Pacific Ocean, Ref.[11,2] (see Fig. **1b**), are shown. The photo in Fig. **1a** was made from the distance of ~200 km away from the center of a thunderstorm, the photo Fig. **1b** – from the distance of ~1600 km. In both cases, as well as in all others, the altitude of the luminous area is estimated in limits of 80÷90 km. Such flashes have obtained the name "elves".

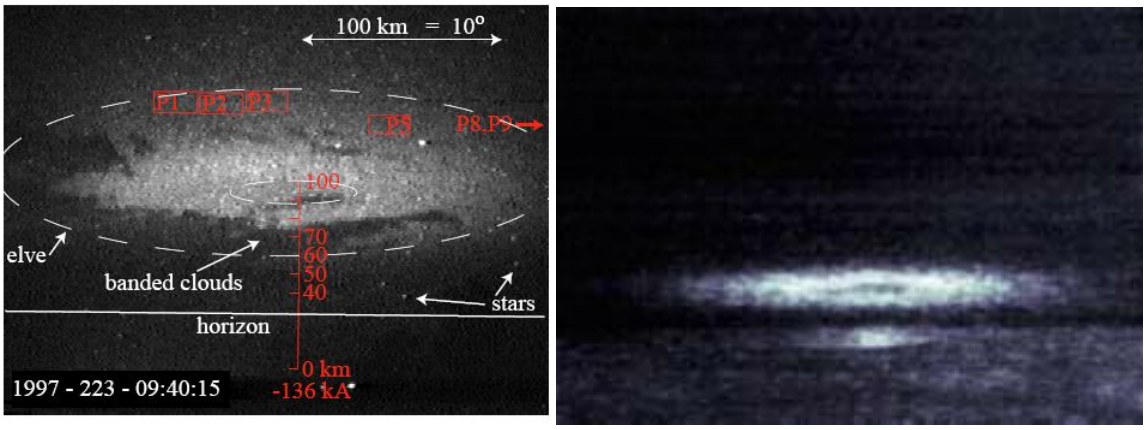

Fig. 1. Photos of the elf: (a) - from a surface of ground made in America, (b) - from shuttle Columbia made in January 2003, h=88±8km

In some cases, probably, at especially strong thunderstorm, on the bottom surface of the elf the large-scale cone-shaped asperities with the spatial period and amplitude about a depth of the luminous area grow. The photo of such formations is given in Fig. **2,** Ref.[10]. From ends of the cones the descending discharge filament structures grow, falling down to an altitude of ~ 40 km. Development of cones and branching of the filamentary structure occurs during 10-20 ms at already extinguished elf. A speed of the filamentary structures front is usually $10^{8\div9}$cm/s. The cones and filamentary structures have a name "sprites".

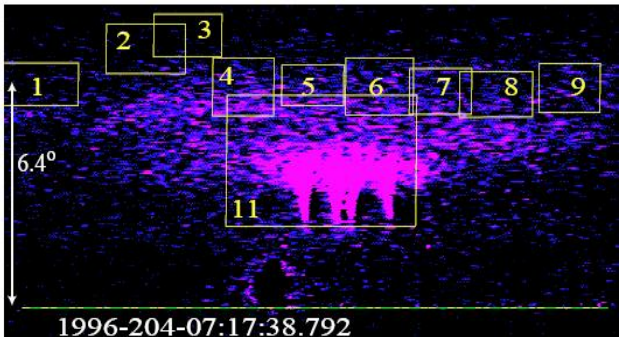

Fig. 2. Fast growth of large-scale regular hills

Dynamics of consecutive development of the elf and sprites one can see in Fig. **3a,** Ref.[12] and Fig. **3b,** Ref.[13]. It is possible to see, that the elf bottom border is moving downwards by 1-2 km during the time of ~1.5 ms, that is, with the speed of ~10^8 cm/s. The front of sprites goes downwards, moving with the speed of ~10^9 cm/s.

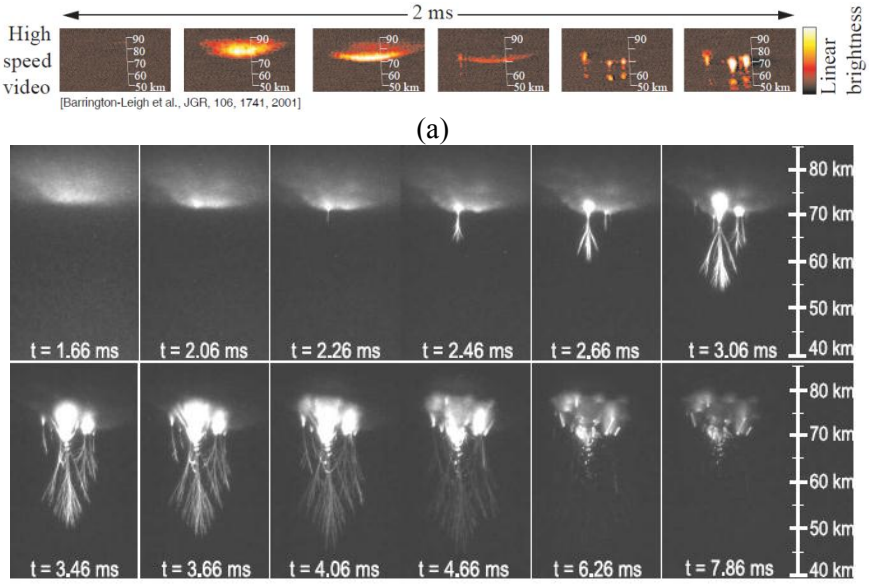

Fig. 3. Dynamics of transition from elf to sprites on the data Ref.[12] - (a) and Ref.[13] - (b)

A photo of one of the powerful sprites is shown in Fig. **4,** Ref.[14]. Temporal evolution of the elf into sprites is well seen in Fig. **5** where a luminosity waveform of all the discharge area is given.

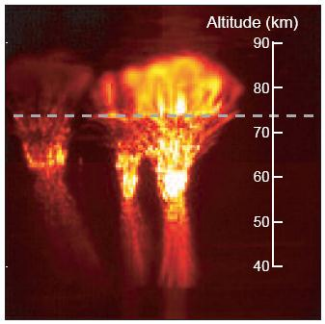

Fig. 4. A photo of the sprites, Ref.[14,19]

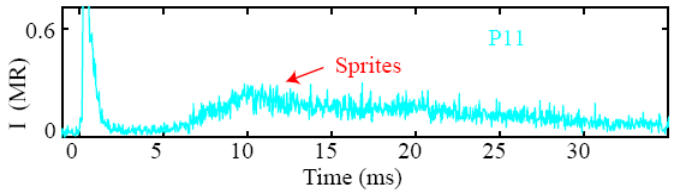

Fig. 5. Oscillogram of a luminescence of all discharge area of elf and sprites, Ref.[10]

The first peak of luminosity during a part of a millisecond corresponds to the elf, the subsequent luminosity during 30 ms – to the sprites. Research of high-altitude discharges was executed also from the specialized satellites, for example, from the satellite DEMETR[15]. With the purpose of UV and IR parts of the flashes spectrum registration the satellites "Tatyana – 1" and "Tatyana – 2" [16,17] were launched. These satellites have brought distributions of flashes over the Earth surface, Fig. **6**. Flashes occur mainly in an equatorial zone (altitude less 30°) not only above continents, where a storm activity is the greatest, but seldom also above the oceans.

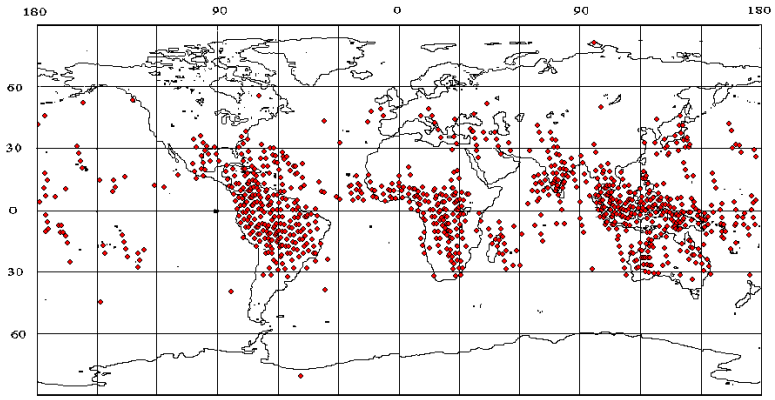

Fig. 6. Observations of flashes UV and IR radiations on the night side from "Tatyana - 2" [16,17]

For an explanation of high-altitude discharges an assumption of an initiating role of powerful lightning discharges[18] and a supposition about a streamer mechanism of filamentary discharge formations development[9] is usually used. At that separate sides of the phenomenon without due quantitative analysis of the process as a whole are discussed.

Thus there are many questions left open:

- how does the initiation of ionization processes in the elves occur,
- why are large-scale formations on their bottom border arising,
- what is a mechanism of the filamentary discharges initiation in the sprites,
- why does the sprites development occur during a time, essentially exceeding the duration of lightning discharges, etc.

For the answer to the put forward questions it was necessary

- to find out all the dynamics of electric and electromagnetic fields behavior during a thunderstorm,
- basing on experience of laboratory discharges observations in similar conditions, to carry out numerical calculations of ionization processes in the mesosphere,
- basing on obtained results, to present a possible scenario of the sprites development proved by quantitative estimations.

The carried out calculations and estimations have allowed to clear all a picture of the phenomenon "elf - sprites" at the quantitative level, having constructed the elementary model suitable for further specifications and complications.

2. The Elementary Model of Atmosphere Ionization by Solar UV Radiation (Layer E and Lower)

The calculations carried out earlier for determination of altitudes where the electric field generated by lightning discharges can exceed a critical value (a value at which excess the avalanche ionization takes place) assume an absence of the conductivity below the ionosphere. At the same time it is known that the regular current with the average density of $\sim 10^{-16}$A/cm^2 flows through the atmosphere from the terrestrial surface to an ionosphere; it assumes the electric conductivity presence. Its presence can have an essential effect on a spatial - temporal distribution of the electric field above the storm cloud.

For determination of the conductivity distribution over the altitude in the atmosphere we will use an elementary model of an ionization balance at which UV radiation of Sun and cosmic rays are present as sources of the ionization.

Let's assume, that a distribution of air molecule's concentration $N(h)$ over the altitude h is described by the barometric formula (we neglect a variation of air temperature with altitude for simplicity)

$$N(h) = N_o \exp\left(-\frac{h}{h_0}\right), \quad h_0 = \frac{k_B T_{av}}{M m_n g} \approx 7.4 km, \qquad (1)$$

here m_n - mass of a neutron, $M = 29$ - molecular weight of the air mixture, which structure is almost constant up to the altitude of 200 km, g - acceleration of gravity, κ_B - Boltzmann constant, T_{av} =245K– average air temperature at altitudes 0÷120 km. Equation (1) approximates air density dependence on altitude relatively standard atmosphere data with accuracy better ±50% for altitudes less 120 km. It is quite enough for our investigation.

Absorption of the Sun radiation J_λ with a wavelength λ in the atmosphere due to the photoionization is described by the Eq.(2)

$$\frac{dJ_\lambda}{dh} = S_{UV}(\lambda)\cdot N(h)\cdot J_\lambda, \tag{2}$$

where $S_{UV}(\lambda)$ is cross-section of photoionization.
The integration of Eq.(2) gives

$$J_\lambda(h) = J_{\lambda_0}\exp\left(-S_{UV}(\lambda)\cdot h_0\cdot N_0\exp\left(-\frac{h}{h_0}\right)\right) \tag{3}$$

where $J_{\lambda 0}$ is origin Sun radiation spectrum density.

Respectively, the source of the ionization is equal to

$$\Psi_{UV_\lambda} = \frac{dJ_\lambda(h)}{dh} \tag{4}$$

After the substitution of the Eq.(3) in Eq.(4) and differentiation it, one gets

$$\Psi_{UV_\lambda}(h) = J_{\lambda_0}\cdot S_{UV}(\lambda)\cdot N_0\exp\left(-\frac{h}{h_0}\right)\cdot\exp\left(-S_{UV}(\lambda)\cdot N_0\exp\left(-\frac{h}{h_0}\right)\right) \tag{5}$$

An effective photoionization cross section can be represented as [19]

$$S_{UV}(\lambda)\approx S_0\lambda^3, \quad \lambda<\lambda_m=\begin{Bmatrix}77\to O_2\\ 80\to N_2\end{Bmatrix}, \ nm$$
$$S_0 = 10^{-24}, cm^2/nm^3 \tag{6}$$

A spectral density of UV radiation with the wavelength shorter than 80 nm, generated, basically, by the Sun crown, is represented in Fig. **7,** Ref.[20].

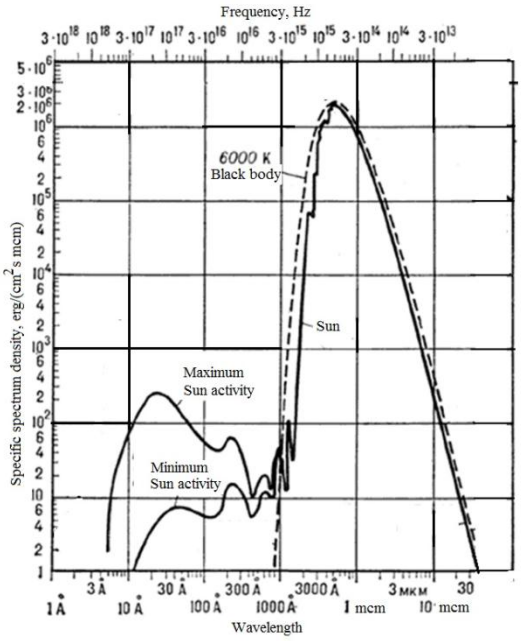

Fig. 7. Spectral density of radiation of the Sun, Ref.[20]

It can be approximated by the black body dependence with the appropriate temperature:

$$I_{UV}(\lambda) = \frac{I_0}{\left(\frac{\lambda}{\lambda_0}\right)^4\left(\exp\left(\frac{\lambda_0}{\lambda}\right)-1\right)}, \quad \frac{1}{cm^3 s} \qquad \lambda_0 = \frac{\hbar 2\pi c}{k_B T_{cor}} = 100nm$$
$$T_{cor}\approx 100eV, \qquad I_0 \approx 3\cdot 10^6\frac{1}{cm^2\cdot s\cdot nm} \tag{7}$$

The value I_0 corresponds to the average between a maximum and a minimum of the Sun activity.
The source of ionization by UV radiation is determined by integral:

$$J_{UV}(h) = \int_{0_1}^{\lambda_m} I_{UV}(\lambda) S_{UV}(\lambda) N(h) \exp\left(-S_{UV}(\lambda) N(h) h_0\right) d\lambda, \quad \frac{1}{cm^3 s} \tag{8}$$

The dependence of the ionization source by UV radiation on altitude is shown in Fig. **8.**

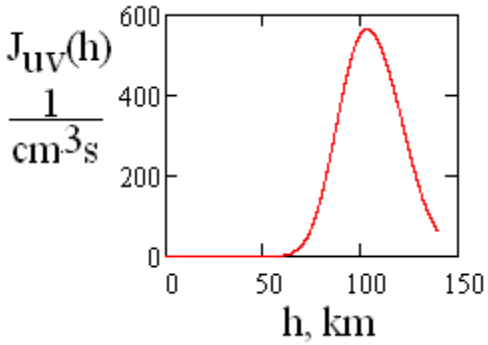

Fig. 8. Dependence of a source of ionization UV radiation from altitude

It is known, that the regular electric current proceeds through all altitudes[21]; at regular electric field at surface of the Earth ~1 V/cm

$$I_{reg} = 2 \cdot 10^{-16}, \quad A/cm^2 \tag{9}$$

Necessary regular conductivity at surface of the ground is supported by cosmic rays. In the assumption of high penetrating ability of space beams the source of ionization by space beams can be approximated by dependence:

$$J_{rays}(h) = C_{rays} \frac{N(h)}{N(0)}, \qquad C_{rays} \approx 2, \quad \frac{1}{cm^3 s} \tag{10}$$

These factors (UV radiation of crown and cosmic rays) are sufficient for maintenance of the *E*-layer and weak ionization of mesosphere and stratosphere. At large altitudes and in polar areas the processes of ionosphere formation are determined by events in magnetosphere too. For their description the more complicated models are required.

Ionization balance of stratosphere, mesosphere and ionosphere is defined by three equations: balance of positive ions, balance of negative ions and a condition of charges quasi neutrality

$$\begin{aligned} &J_{UV}(h) + J_{rays}(h) - \beta_i \cdot n_+ \cdot n_- - \beta_e \cdot n_+ \cdot n_e = 0 \\ &\left(K_a(T_e) + K_3(T_e) \cdot N(h)\right) \cdot N(h) \cdot n_e - \beta_i \cdot n_+ \cdot n_- = 0 \\ &n_e + n_- - n_+ = 0 \end{aligned} \tag{11}$$

where $\boldsymbol{\beta_{e,i}}$ - coefficients of electron - ion and ion – ion recombination, $\boldsymbol{K_a}$ and $\boldsymbol{K_3}$ - constants of dissociation and three-body attachment reactions, depending on electron temperature, which are determined by ratio of electric field and gas concentration *E/N*. Solution of system (11) is shown in Fig. **9.**

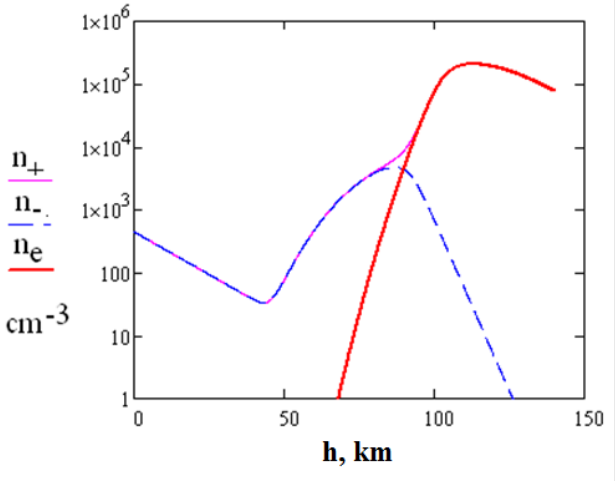

Fig. 9. Day time distribution of concentration of ions and electrons on altitude

At night ***E***-layer is recombining

$$n_{e_{night}}(t) = \frac{n_{e_{day}}}{1 + n_{e_{day}} \beta_e t} \tag{12}$$

In Fig. **10** the calculated distributions of electron concentration for day time and night time are compared with well-known results of observations[22]. The satisfactory agreement for the altitudes up to 150 km (layer *E* and lower) certifies applicability of used elementary model for the further analysis.

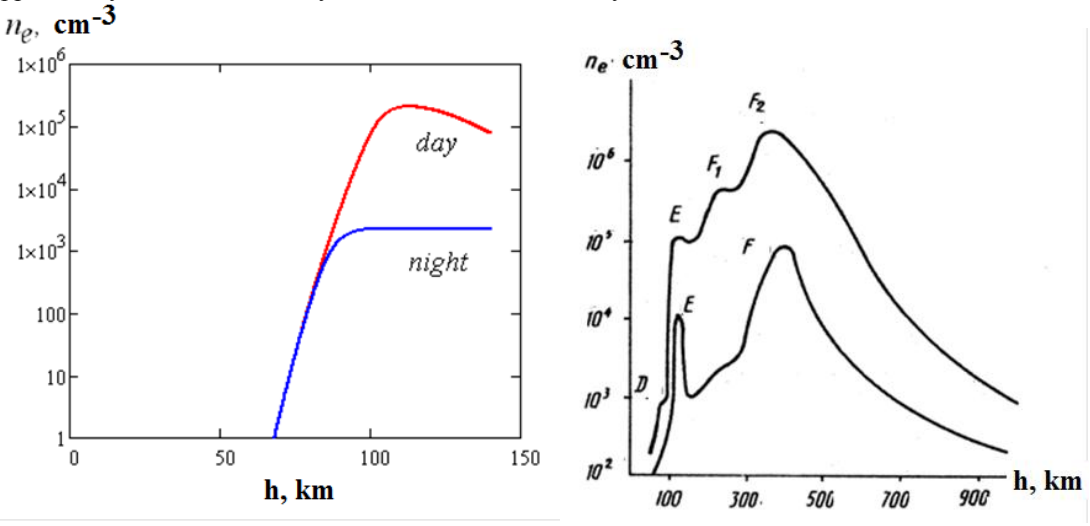

(a) **(b)**

Fig. 10. Distribution of electronic concentration in the afternoon and at night: (a) – the calculation result, (b) - the data of measurements.

Basing on the obtained distributions of ion and electron concentrations, it is not difficult to calculate the appropriate conductivity with the account of magnetic field influence

$$\sigma_\alpha(z) = \frac{n_\alpha(z) e^2}{m_\alpha \nu_{tr_\alpha}(z) \sqrt{1 + \left(\frac{\omega_{H_\alpha}}{\nu_{tr_\alpha}(z)} \right)^2}}, \tag{13}$$

$$\nu_{tr_\alpha}(z) = K_{tr} \left(\frac{E}{N(z)} \right) N(z)$$

and their sum

$$\sigma_{tot}(z) = \sum_\alpha \sigma_\alpha(z) \tag{14}$$

Index α corresponds to negative ions, positive ions or electrons, $K_{tr\alpha}$ is constant of transfer collisions of particles α.

The distributions of the total and the separate conductivities are shown in Fig. **11.**

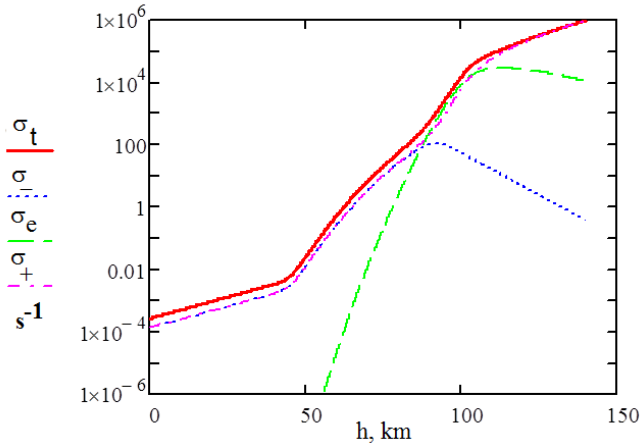

Fig. 11. Electric conductivity distributions on altitude: dotted line - electronic conductivity, points - conductivity of negative ions, stroke - dotted line - positive ions, and continuous line - total conductivity

The regular current through media with the calculated total conductivity, Eq.(14), creates a regular electric field in atmosphere, which distribution is shown in Fig. **12**. The quantitative and qualitative agreement with the observations also confirms applicability of used model.

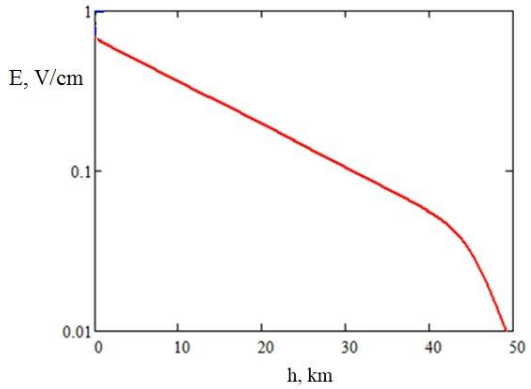

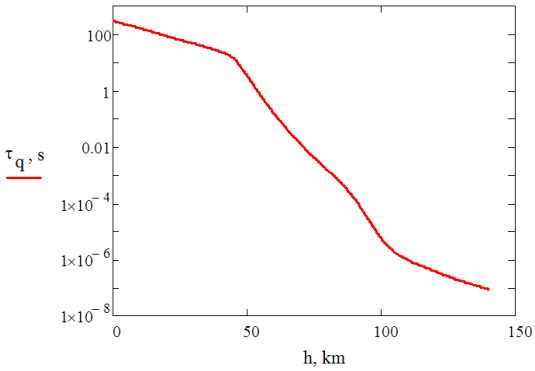

Fig. 12. Distribution of a regular electric field in the atmosphere

Fig. 13. Distribution of a charge relaxation time over the altitude

The relaxation time of the charge, appropriate to the total conductivity, is defined by Eq.(15)

$$\tau_q = \frac{1}{4\pi\sigma_{tot}} \tag{15}$$

It depends on the altitude, varying by many orders of magnitude (see Fig. **13**).

If in troposphere and lower stratosphere this time is of many minutes, then in mesosphere it is of tens milliseconds, and in ionosphere it is of microseconds. As the cloud charging, caused by the convective processes in troposphere, occurs during time, estimated by minutes, the lightning discharge occurs during parts of millisecond, the dynamics of the electric field above cloud demands calculations taking into the account the distribution of electric conductivity over troposphere.

3. Dynamics of an Electric Field Above a Storm Cloud

Slow increase of the cloud charge causes a polarization in stratosphere, mesosphere and ionosphere. Cloud we present as a charged disk with radius L_c, located above a surface of ground at altitude h_0. The lightning discharge occurs on the axis of the cloudy disk (see Fig. **14**). The field of the cloud is determined by the sum of the cloud charge and its reflection under terrestrial surface. The cloud and the ground are considered well conducting.

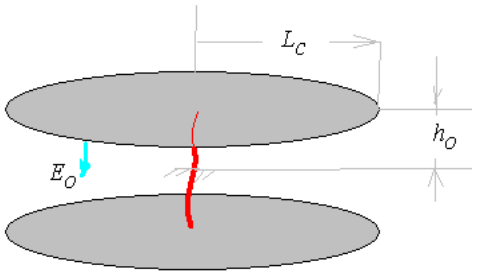

Fig. 14. A cloud and its "reflection"

The potential of the charged disk of radius R_c with charge q in emptiness is defined by Eq.(16)

$$\phi(r,z)=\frac{q}{R_c}\,arctg\left(\sqrt{\frac{2R_c^2}{r^2-R_c^2+z^2+\sqrt{\left(r^2-R_c^2+z^2\right)^2+4R_c^2z^2}}}\right) \tag{16}$$

The potential of the charged disk located above conducting plane at altitude h_0, is equal to

$$\psi(r,z)=\phi(r,z-h_0)-\phi(r,z+h_0) \tag{17}$$

The module of electric field is described by Eq.(18)

$$E_{cloud}(r,z)=E_0\frac{\sqrt{\left(\frac{\partial\psi(r,z)}{\partial z}\right)^2+\left(\frac{\partial\psi(r,z)}{\partial r}\right)^2}}{\sqrt{\left(\frac{\partial\psi(0,0)}{\partial z}\right)^2+\left(\frac{\partial\psi(0,0)}{\partial r}\right)^2}} \tag{18}$$

E_0 - field at the ground under cloud.

The formulae of the Eq. (18) at $r = 0$ with good accuracy is approximated by the expression

$$E^0_{cloud}(z)\approx E_0\left(\frac{h_0^2+L_c^2}{(z+h_0)^2+L_c^2}-\frac{h_0^2+L_c^2}{(z-h_0)^2+L_c^2}\right) \tag{19}$$

Let the cloud field increases by exponential law

$$E_0\sim\left(1-\exp\left(-\frac{t}{\tau_{ch}}\right)\right), \tag{20}$$

where τ_{ch} is a characteristic time of the charging in conducting media. It causes occurrence of polarization field

$$E_{polarization}=E^0_{cloud}(z)\left(\frac{\sigma_{tot}\tau_q\exp\left(-\frac{t}{\tau_{ch}}\right)-\exp(-\sigma_{tot}t)}{\sigma_{tot}\tau_q-1}-1\right) \tag{21}$$

where τ_q is defined by Eq.(15)

The resulting field of cloud before lightning discharge is defined by the sum

$$E_{before}=E_{cloud}+E_{polarization} \tag{22}$$

The field in atmosphere before lightning discharge depending on altitude is shown in Fig. **15** (r = 0, E_0 = 500 V/cm, τ_{cloud} = 3000 s).

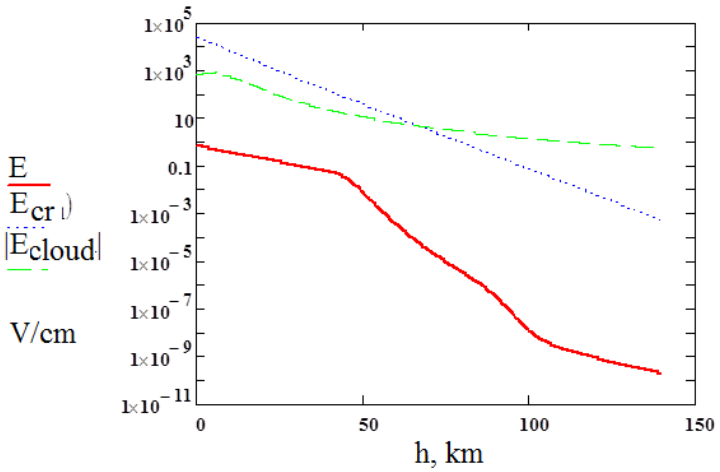

Fig. 15. Distributions of: the field of the cloud before lightning discharge - continuous line, the field of the cloud without taking into account conductivity of air - dashed line, the critical field - a dot line.

At all altitudes, electric field is much smaller than critical value, which for simplicity is approximated by Eq.(23):

$$E_{cr} = 25 \cdot \exp\left(-\frac{h}{h_0}\right), \quad kV/cm \tag{23}$$

After the lightning discharge the charge of cloud becomes small and only polarization field rests in the atmosphere, which slowly relaxes with local value of characteristic time Eq.(15). This field is kept in the stratosphere and the mesosphere tens and hundreds milliseconds. In mesosphere at altitudes 70÷90 km the electric field exceeds critical value during ten milliseconds. In Fig. **16** the field of polarization and its relation to critical value at various moments of time after lightning discharge are shown.

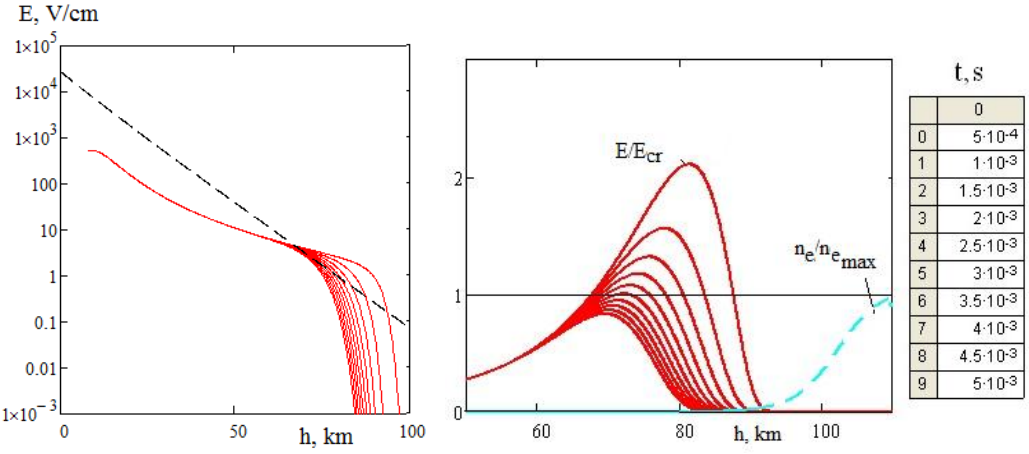

(a) (b)

Fig. 16. A field of the polarization - (a), and its relation to the critical value - (b). The moments of the time after the lightning discharge are specified in the table. The curves are numerated downright.

After lightning discharge of the storm cloud at bottom border of E-layer a zone of overcritical fields has appeared. Its radius can exceed a hundred kilometers. In Fig. **17** the distribution of the overcritical field zone, calculated with using of the Eq.(18) for the time moment 0.5ms after the lightning discharge, is shown.

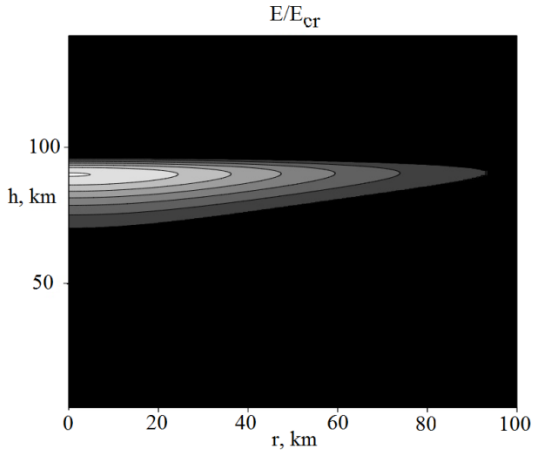

Fig. 17. The area overcriticality of the electric field after lightning discharge of the storm cloud

The size of the overcritical field zone is quite well coordinated with the observations (see. Fig. **1a**). The overcriticality (E/E_{cr} >1) is retained during several milliseconds with respect to local value of electric conductivity. Lower area of overcriticality (h < 65 km) the electric field is smaller than critical one in several times.

Since electromagnetic wave pass-time between ground and ionosphere (~ 3 ms) is comparable with duration of lightning discharge (<1 ms), the qualitative conclusion on the polarization field role in the process, obtained by the calculations carried out in the electrostatic approximation, require a verification within the framework of electrodynamics.

3.1.*Numerical Modeling of the Electromagnetic Field Generation During Cloud Charging and Lightning Discharge*

The dynamics of the electromagnetic field in the vicinity of the storm cloud during a slow charging of clouds and after lightning discharge was investigated numerically. In contrast to the previous researches (see, for example, Ref.[23, 10]) the model takes into account a small, but final, conductivity of the stratosphere and mesosphere and the stage of a slow cloud charging.

The problem formulation is shown in Fig. **18.**

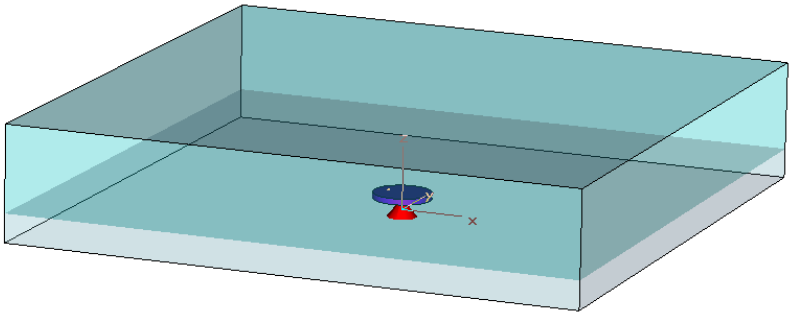

Fig. 18. The geometry of the task statement on modeling of electromagnetic field dynamics in a vicinity of the storm cloud during slow charging cloud and in time and after the lightning discharge

Between the ionosphere and the ground surface, which conductivity is assumed to be high, at the altitude of 8 km the disk shaped conducting "cloud" is located. Above 20 km the area with final small conductivity is disposed. The slow charging of the "cloud" under the linear law during the time of several seconds is interrupted by the short circuit through the lightning channel with the known conductivity, connecting the "cloud" with the ground. 3D calculations of the electromagnetic field was carried out with a help of the standard code.

In Fig. **19** a dependence of the lightning current magnetic field on time in the point located at the altitude of 1 km, at the distance of 1 km from the lightning channel, is shown. The maximum of the magnetic field corresponds to the maximum current in the lightning channel equal to 13 kA. The discharge current in the lightning channel has duration about of 0.5ms.

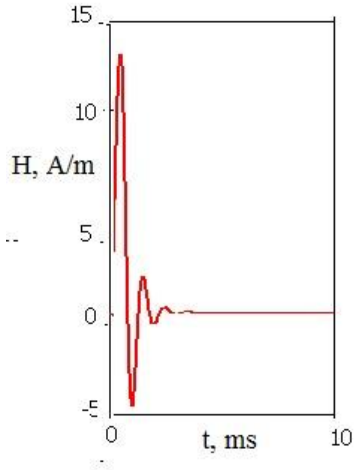

Fig. 19. The field H at the altitude 1 km at the distance of 1 km from the lightning channel

In Fig. **20** a dependence of the electric field on time above the cloud for various values of the altitude is submitted.

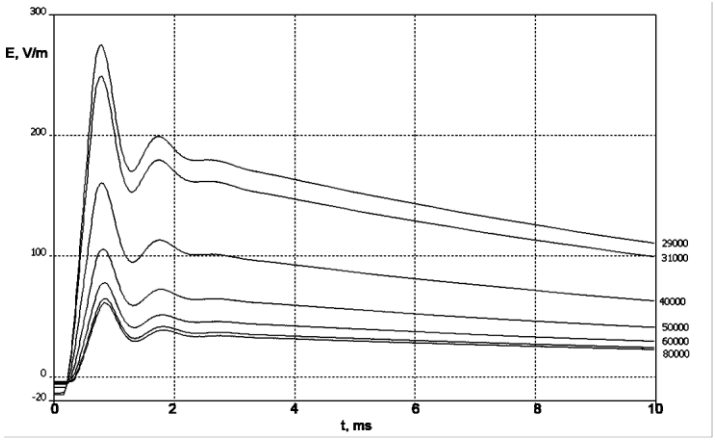

Fig. 20. A dependence of the electric field on time above the cloud for various values of the altitude. Figures at curves – the altitude in meters.

Though the lightning discharge was finished during the time smaller than 1 ms, and the generation of the electromagnetic dipole radiation has been finished, the electric field above the cloud under the ionosphere at all the altitudes continues to exist during tens of milliseconds. This polarization field is caused by the separation of charges during the slow charging of the cloud. The electromagnetic wave, which has brought in its contribution to the maximum of the field above the cloud, divergences radially in the waveguide channel, formed by ground and ionosphere, having left a zone with a radius of 100km during the time about of 1ms. In Fig. **21** spatial distributions of the electric field at the bottom border of the ionosphere after 1ms - (a) and 10ms - (b) from the moment of the lightning discharge beginning are shown.

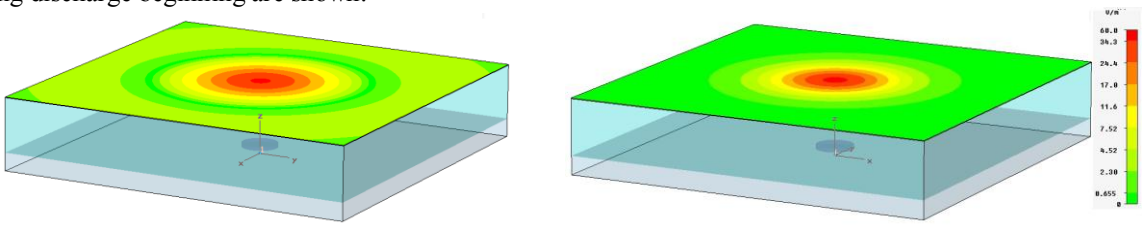

(a) (b)

Fig. 21. Spatial distributions of the electric field at the bottom border of ionosphere after 1 ms - (a) and 10 ms - (b) from the moment of the lightning discharge beginning

Thus, the numerical modeling has confirmed that at the accounting of the finite conductivity of the space between the ionosphere and the cloud in the zone with the radius about of 100 km the electric field after the lightning discharge is retained during tens of milliseconds**.**

3.2*Appearance of the plasma layer on the bottom border of the ionosphere*

An excess by several times of the electric field over the critical value at the altitudes of 70 – 90 km, arising after the lightning discharge, causes quick ionization in this zone. The research of this process we will carry out by the numerical modeling in 1D statement with using of the data about the electrical conductivity of the atmosphere obtained above and the expressions of Eq.**(19)** for the modeling description of the storm cloud' initial field distribution over the altitude, which scheme is submitted in Fig. **13**.

The dynamics of the process is described by the system of Eq.(24), where designations are entered by the Eq.(25) . Rate constants of the dissociative attachment $K_a(E/N)$, and the ionization by the electron impact $K_i(E/N)$ reactions and the coefficients of the ion - ion β_i and the ion - electron β_e recombination are taken for the air mixture

$$\begin{cases} \dfrac{\partial n_-}{\partial t} = K_a\left(\dfrac{E}{N(z)}\right)N(z)n_e - \beta_i n_- n_+ \\ \dfrac{\partial n_+}{\partial t} = K_i\left(\dfrac{E}{N(z)}\right)N(z)n_e - \beta_e n_e n_+ + \Psi(z), \\ n_e = n_+ - n_- \\ \dfrac{\partial E}{\partial t} = -4\pi\sigma_{tot}(z)E + \dfrac{\partial E_{cloud}(z,t)}{\partial t} \end{cases} \tag{24}$$

where $\sigma_{tot}(z)$ is defined by the Eq.(14) and Eq.(13).

The own field of the cloud firstly rises during its charging up to the moment of time t_0, after which the lightning channel connects the cloud with ground. The resonant counter, formed by cloud capacity and lightning channel inductivity starts the damping oscillations at the law given by Eq.(25)

$$E_{cloud}(z,t) = E^0_{cloud}(z)\begin{cases} \left(1 - e^{-\frac{t}{\tau_{ch}}}\right), & \text{if } t<t_0 \\ \cos\left(\Omega(t-t_0)\right)e^{-\delta\Omega(t-t_0)}, & \text{if } t>t_0 \end{cases} \tag{25}$$

Here

$$\Omega \approx \frac{c}{L_c\sqrt{\pi \cdot \ln\left(\dfrac{2h_0}{a_{ld}}\right)}} \tag{26}$$

Is the own frequency of the contour, determined by geometrical parameters of the model (see Fig. **14**), a_{ld} is the lightning channel radius, c – light velocity, δ - decay factor of oscillations, caused by finite conductivity of the lightning channel. Decay factor is chosen equal to 0.4. In Fig. **22** dependences of the own electric field of the cloud (a) and the current in the lightning channel (b) are shown at $t > t_0$.

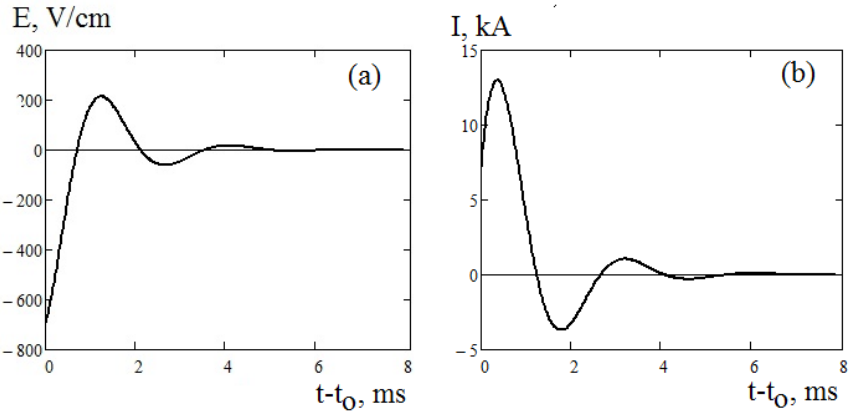

Fig. 22. Dependences of the own electric field of the cloud on the ground – (a) and a current in the lightning channel –b.

Results of the modeling are submitted in Fig. **23**.

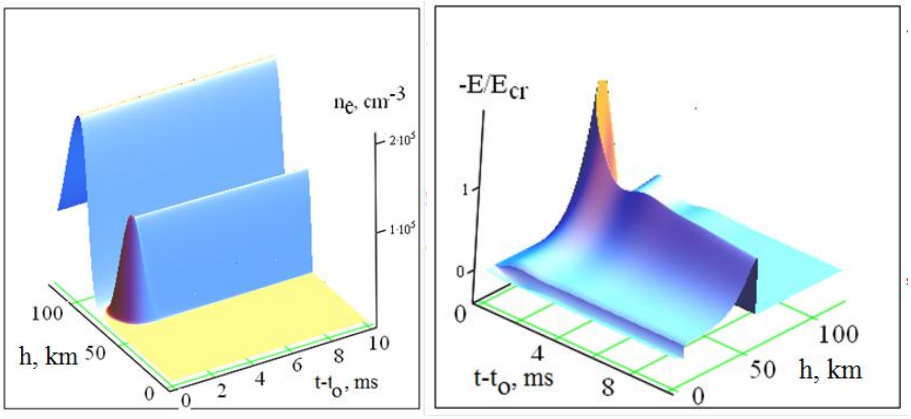

(a) (b)

Fig. 23. The ionization in the zone of the electric field overcriticality: the electron concentration - (a), the electric field - (b)

As one can see, under the bottom border of the ionosphere during the time of the lightning discharge the layer of the ionization appears, which is kept for a long time. The electric field inside the arisen layer is small, so the dissociative attachment ceases to play an appreciable role. The three-body attachment also is insignificant, as the concentration of molecules is small at the altitudes of the ionization layer generation. The layer lifetime is defined by the recombination and as long as hours. Occurrence of the ionization layer has a character of an avalanche of the ionization, which moves downwards with a speed about of 10^8cm/s, until it does not reach the border of the overcriticality region. The arisen layer of the ionization fills all overcriticality zone (see. Fig. **16**). A luminosity of the ionization area, caused by the excitation of molecules by hot electrons, takes place if the electric field is comparable with the critical one and the electron temperature, dependent on parameter *E/N*, is sufficient for the excitation of molecules. It is natural to assume, that the intensity of radiation is proportional to the specific power of its ohm heating. The integration over the layer depth gives dependence, from which follows that the luminescence precedes only during the development of the avalanche and stops at its arrival to the border of the overcritical area. This time has a value about of 1 ms. The luminosity of the ionization area at the altitude of 70-90 km arising during the thunderstorm at duration about of one millisecond, is associated with the observations of "elves".

Though the arisen layer of the ionization stops to shine, the long existence of its high ionization level influences the distribution of the electric field and the further events.

4. The Mechanism of the "Sprites" Occurrence

The front of avalanche ionization is unstable with respect to large-scale perturbances of its surface [24]. Any asperity on a flat surface of a capacitor plate results in an increase of electric field on the asperity. The speed of ionization avalanche is defined by Eq.(27)

$$V_{fr} = 2\sqrt{D_e\left(\nu_i - \nu_a\right)} \tag{27}$$

where $\boldsymbol{D_e}$ is the coefficient of free electronic diffusion [25], and

$$\nu_a = K_a\left(\frac{E}{N(z)}\right)N(z) \tag{28}$$

is the frequency of the dissociative attachment; and

$$\nu_i = K_i\left(\frac{E}{N(z)}\right)N(z) \tag{29}$$

is the frequency of the ionization by the electron impact. The greater asperity, the faster it grows. Since the frequency of the ionization is a growing function of the electric field, then the speed of exserted part of the front exceeds the speed of the not exserted part.

For estimation, we approximate the form of the asperity by the half of the ellipsoid of revolution with the symmetry axis directed normally to the surface of the ionization avalanche front, see Fig. **24a**.

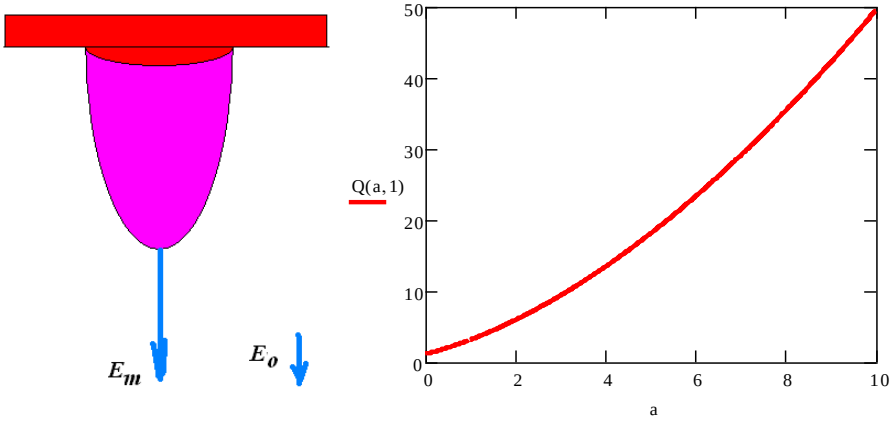

(a) (b)

Fig. 24. An approximation of the form of a protuberance - (a), dependence from the Eq.(30) at b =1 - (b)

The conductivity of the layer, as the calculations stated above show, is high enough for full shielding of the electric field during the time of the microsecond order. Therefore for the estimation of the field increase at the top of the asperity, it is possible the layer and the asperity to consider as ideally conducting and to apply the known formula for the ideally conducting ellipsoid of revolution located in the external field represented by Eq.(30)

$$Q(a,b) \equiv \frac{E_m}{E_0} = \begin{cases} \dfrac{2e_{long}^3}{1-e_{long}^2} \cdot \dfrac{1}{\ln\left(\dfrac{1+e_{long}}{1-e_{long}}\right) - 2e_{long}}, & e_{long} = \sqrt{1-\left(\dfrac{b}{a}\right)^2}, \quad a>b \\ \dfrac{e_{flat}^3}{1+e_{flat}^2} \cdot \dfrac{1}{e_{flat} - arctg\left(e_{flat}\right)}, & e_{flat} = \sqrt{\left(\dfrac{b}{a}\right)^2 - 1}, \quad a<b \end{cases} \tag{30}$$

Here ***b*** is the radius of the basis of the ellipsoidal asperity, ***a*** is its height. The dependence, given by the Eq.(30), is shown in Fig. **24b**.

Having applied for simplicity the known approximation of the ionization and the dissociative attachment sum of frequencies[26].

$$\nu_i - \nu_a = \nu_a \left(\left(\frac{E}{E_{cr}} \right)^{\beta} - 1 \right), \qquad \beta \approx 5.34, \tag{31}$$

and using the Eq.(27), we estimate the speed of the asperity development in the coordinates of the front

$$\frac{da}{dt} = V_{fr} \left(\frac{\sqrt{\left(\dfrac{E}{E_{cr}} Q(a,b) \right)^{\beta} - 1}}{\sqrt{\left(\dfrac{E}{E_{cr}} \right)^{\beta} - 1}} - 1 \right) \tag{32}$$

For small values of ***a*** the approximation is fair

$$Q(a,b) \approx 1 + \frac{\pi}{2}\frac{a}{b}, \quad a<<b. \tag{33}$$

With taking into account of Eq.(33), it is easy to receive the increment of the asperity development

$$\gamma_{\max} \approx \frac{V_{fr}}{b}\frac{\beta}{4}\left(E/E_{cr}\right)^{\beta} \tag{34}$$

The small-scale heterogeneity of the electron concentration in the bottom of the ionosphere with the horizontal sizes from several hundred meters up to tens kilometers are formed as a result of the turbulence caused by numerous reasons (winds, magnetosphere electric currents, gravity-acoustic waves and so on)[27]. The relative intensity of small-scale electron density fluctuations altitudes from 80 km up to 400 km is estimated by the value about of 10^{-2}. Assuming

$$V_{fr} = 10^8 \ km/s, \quad b = 3 \ km, \ E/E_{cr} = 1.5, \ a(t=0) = 0.03 \text{ km}, \tag{35}$$

we get the estimated value of the increment $\gamma \approx 10^4$ s^{-1}. However, with the growth of the asperity the overcriticality E/E_{cr} at its top grows. Respectively, the increment grows. In the nonlinear case the development is defined by Eq.(32). Its solution for the considered case, given in Fig. **25,** has the explosive character.

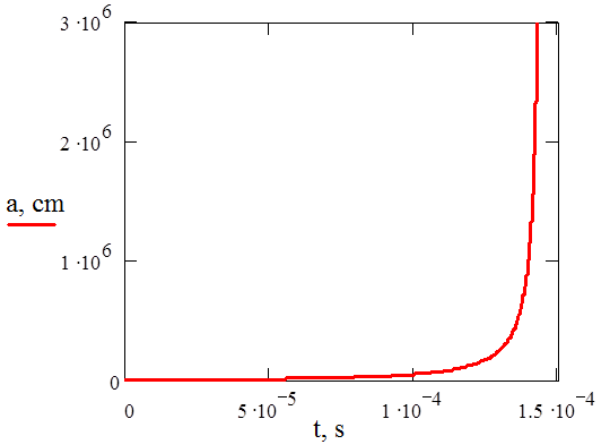

Fig. 25. The solution from the Eq.(32) for the conditions (35) , describing the development dynamics of "sprite"

After the time about of 100 μs the slow growth is replaced by the sweeping development and for ten microseconds the asperity grows up to 30 km.

In real conditions the front of the ionization still moves within the limits of the zone of the overcritical field while the top of the asperity is already in the far subcritical field.

There can be several such asperities, caused by ionization front instability. They are the observed phenomena such as "sprites" (see Fig. **2** and Fig. **3**). We have to note, that the "elf" already is extinguished since its bottom front has reached the border of overcriticality and the electric field in it is relaxed already. But the "sprites" brightly shine, since their growth is accompanied by the acting of the current which is taking out a charge from the ionized layer of elf to tops of the asperities.

The electric field at the top of the individual asperity, which has reached the altitude ***h***, remains at all the altitudes greater than of the critical value (curve (c) in Fig. **26**). However, in the system of the asperities the field at their tops grows with their length up to the length comparable with the distance between them. For the system of the asperities the field at their tops exceeds the critical one up the altitudes ***h***, which is not lower than of some definite value (a curve (b) Fig. **26**)

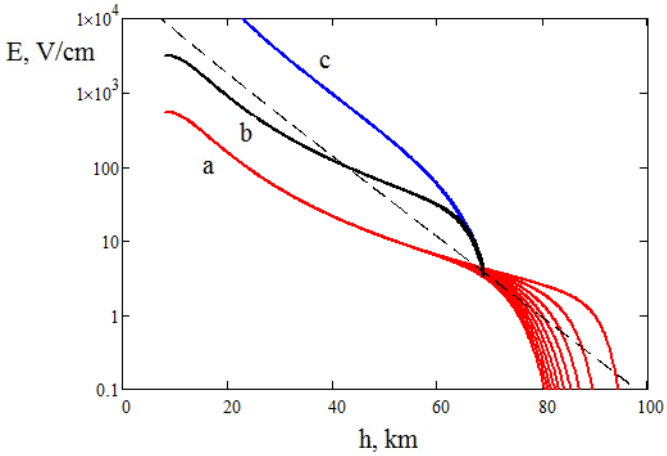

Fig. 26. A dependence of the electric field on altitude: (a) - the field under the layer of ionization in the absence of protuberances (the same, that on Fig.6.15), (b) - a field at tops of system of the protuberances, (c) - the field at the top of an individual protuberance, a dotted line - the critical field

During the development process the sharp peaks of the asperities initiate networks of thin streamer channels (see Fig. **27,** Ref.[7]), playing a role of the initiator, without which the streamer discharge cannot appear in the subcritical field. Though the lightning discharge and the electromagnetic field, caused by it, were finished, the discharge processes proceed in the field of the polarization, getting from it energy necessary for the ionization and the heating of channels.

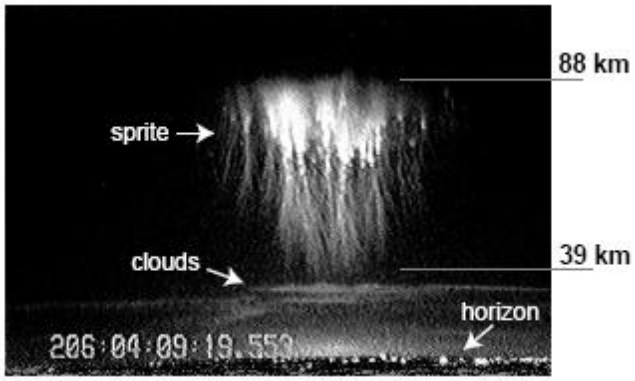

Fig. 27. Streamer channels initiation by the large-scale protuberances [7]

On the streamer nature of the filament structures, being the continuation of the large-scale asperities, it was indicated already in Ref.[28]. However, the question about an initiation of the streamer discharge in the subcritical field remained open. As the initiators the tracks of the high energy cosmic particles, the meteoric traces, and even the "running up electrons"[29] were attracted.

Presence of the large-scale asperities, reliably providing the initiation of the streamer channels, makes other factors not necessary.

The phenomenology of the streamer subcritical discharges is investigated in detail enough. Their development can be accompanied by the multiple branching as one can see in Fig. **28,** Ref.[10].

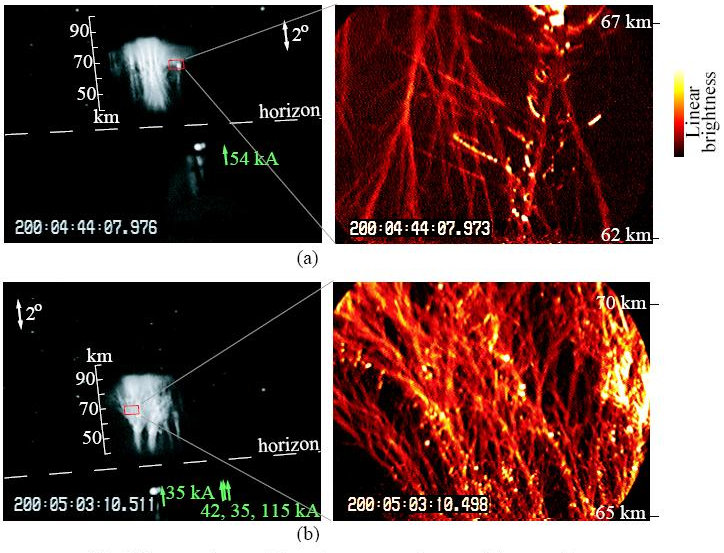

Positive and negative streamers in positive sprites.

Fig. 28. Branching of channels in the streamer discharge [10]

Unlike the streamer subcritical discharges in the microwave (MW) field, which form no less complex networks of the filament channels (see Fig. **29**), the streamer subcritical discharge in the quasi-stationary electric field cannot leave the initiator, scooping from it the electric charge necessary for the development. But the streamer heads, also as the MW streamer discharge, are the powerful source of the UV radiation.

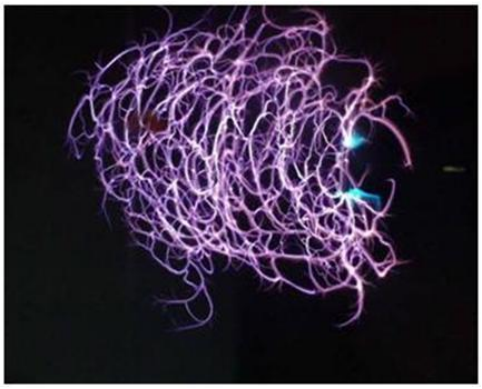

Fig. 29. Network of streamer channels in the MW streamer subcritical discharge.

Namely the streamer phase of the "sprites" generates the flash of the UV radiation, registered by the equipment of satellites, in particular the satellites "Tatyana - 1" and "Tatyana - 2"[17].

In Fig. **30** the spectrum of sprites radiation, registered by the ground detector[10] and the spectrum of the MW streamer subcritical discharge, observed in laboratory conditions, are compared.

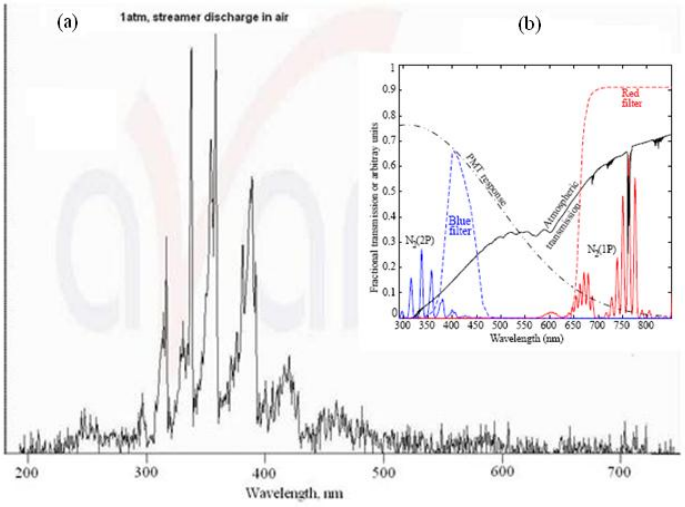

Fig. 30 Spectra of radiation: (a) - the spectrum of the MW streamer subcritical discharge, (b) – the spectrum of the "sprites, Ref.[10]

In the short-wave area the spectra are practically similar, that confirms the similarity of the processes in the streamer channels, in their head part, specifying their spark nature.

5.Conclusion

The slowly increasing charge of the cloud causes the polarization in the atmosphere. Redistribution of charges in the atmosphere neutralizes the field of the cloud. After the lightning discharge the residual field of the polarization, relaxing for a long time, stays.

At the sufficiently strong thunderstorm, this field exceeds the critical value on the bottom border of the ionosphere. There originates the avalanche of the ionization moving downwards with the speed of 10^8-10^9cm/s. It is the "elf".

The front of the avalanche ionization is unstable with respect to the growth of the asperities with the sharpening tops. The size of the bases of the asperities is determined by the depth of the avalanche front. When the asperities reach a zone of the subcritical field, at tops of the asperities the systems of the streamer channels appears, sufficiently thin for ability of development in the deeply subcritical field.

The relaxation time of the electric field is great enough for the development of process during tens of milliseconds. The asperities with the attached streamer channels net are the “sprites”.

Filamentation of the polarization currents at the altitude higher than 120 km creates the flash of IR radiation. The bright part of the elf and the streamer part of the sprites generate the flash of the UV radiation registered by the satellites.

Acknowledgements.

The author thanks Boris Khrenov who has attracted his attention to the most interesting problem of the high-altitude discharges, and prof. A.A. Rukhadze, for the constructive discussion.

References

[1]. Boeck, W. L., Vaughan, O. H., Blakeslee, R. J., Vonnegut B., Brook M., McKune J.: Observations of lightning in the stratosphere. J. Geophys. Res., 100, D1, 1465-1475 (1994)

2. Boeck W. L.,. Vaughan O. H. Jr., Blakeslee R. J., Vonnegut B. and M. Brook M. The role of the space shuttle videotapes in the discovery of sprites, jets and elves. Jour. Atmos. Sol. Terr. Phys., 60, 669-677. (1998):

3. Franz, R. C., R. J. Nemzek, J. R. WincklerTelevision image of a large upward electric discharge above a thunderstorm system, Science, 249, 48–51 (1990).

4. Sentman D. D., Wescott E. M.. Observations of upper atmospheric optical flashes recorded from an aircraft. Geophys. Res. Lett., 20, 2857–2860 (1993)

5. Lyons W.A.. Characteristics of luminous structures in the stratosphere above thunderstorms as imaged by low-light video. Geophys.Res. Lett., 21, 875–878 (1994)

6. Sentman D.D., Wescott E.M., Osborn D. L., Hampton D. L, Haevner M. J., Preliminary results from the Sprites94 aircraftcampaign 1. Red sprites. Geophys. Res. Lett., 22, 1205–1208 (1995)

7. Steven Andrew Cummer.: Lightning and ionospheric remote sensing using VLF/ELF radio atmospherics. Dissertation on Ph.Dr.StanfordUn. (1997)

8. Pasko V.P., Red sprite discharges in the atmosphere at high altitude: The molecular hysicsand the similarity with laboratory discharges. Plasma Sources Sci. Technol., 16, S13–S29 (2007)

9. Raizer Yu.P., Milikh M., Shneider M. N.. Streamer- and leader-like processes in the upper atmosphere: models of red sprites and blue jets. Journal of Geophys. Res., vol. 115, a00e42 (2010)

10. Christopher Paul Barrington-Leigh.: Fast photometric imaging of high altitude optical flashes above thunderstorms. Dissertation on Ph.Dr., Stanford Un. (2000)

11. Yair Y., Price C., Levin Z., Joseph J., Israelevitch P., Devir A., Moalem M., Ziv B., Asfur M., Sprite observations from the space shuttle during the Mediterranean Israeli Dust Experiment (MEIDEX), J. Atmos. Sol. Terr. Phys., 65, 635–642, 2003.

12. Barrington-Leigh C. P., U. S. Inan, and M. Stanley. Identification of Sprites and Elves with Intensified Video and Broadband Array Photometry. J. Geophys. Res. 106, 1741, (No. 2, February, 2001).

13. Cummer S. A., Jaugey N., Li J., Lyons W. A., Nelson T. E., Gerken E. A., Submillisecond imaging of sprite development and structure, Geophys. Res. Lett., 33, L04104 (2006)

14. Stenbaek-Nielsen H. C., Moudry D. R., Wescott E. M., Sentman D. D., Sabbas F.T.S.. Sprites and possible mesospheric effects, Geophys. Res. Lett., 27, 3829–383 (2000)

15. Błecki J., Parrot M., Wronowski R.. ELF and VLF signatures of sprites registered onboard the low altitude satellite DEMETER. Ann. Geophys., 27, 2599–2605, (2009)

16. Sadovnichiy V.A., Panasiuk M.I., Yashin I.V. et al.: Cosmic media rsearch on microsatellits “University-Tatiana” and “Univercity -Tatiana-2’. Astronomicheskiy Vestnic”, т.45, No.1, с. 1-27. (in Russian) (2011)

17. Veden’kin N.N., Garipov G.K., Klimov P.A., Klimenko V.V., Mareev E.A., Morozenko V.S., Pak I., Panasyuk M., Salazar U., Tulupov V.I., Khrenov B.A., Yashin I.V.. Atmospheric flashes in UV and IR diapasons by data of satellite “University – Tatiana 2”. Zurnal Eksperimentalnoi i Teoretichskoi Fiziki, 140, No. 3(9), 1-11 (in Russian) (2011)

18. Marshall R.A., Inan U.S.. Possible direct cloud-to-ionosphere current evidenced by sprite-initiated secondary TLEs. Geophys. Res. Let., 34, L05806, (2007)

19. Kramers H.A. The law of dispersion of X-ray absorption and of continous X-ray spectrum. Phil. Mag., 46, 836 (1923)

20. I.M.Chertok.. Sun. Fizicheskaia eciklopedia, V.4, p.394. Moscow. (in Russian) (1994)

21. Imianitov I.M., Chubarina E.V.. Electricity of a free atmosphere. L.. (in Russian) (1965)

22. G.S.Ivanov-Kholodny. Ionosphere.. Fizicheskaia eciklopedia, V.2б, p.213. M (in Russian)1994

23. Veronis G., Pasko V., Inan U.. Characteristics of mesospheric optical emissions produced by lightning discharges. Journal of Geophys. Res., 104, No.12, 645-656 (1999)

24. Khodataev K.V.. On avalanche ionization of electronegative gas in DC field. Fizika Plasmy. 21, No.7, 605-610 (in Russian) (1995)

25. Khodataev K.V., Gorelic B.R.. Diffusion and drift regimes of propagation of a flat ionization wave in MW field. Fizika Plasmy. 23, No.3, 236-245 (in Russian) (1997)

26. Mayhan J.T. Comparison of various microwave breakdown prediction models. J. Appl. Physics, 42, 5362-5368 (1971)

27. Gershman B.N., Erukhimov L.M., Yashin Yu.Ya.. Wave phenomena in ionosphere and cosmic plasma., Moscow. Nauka (in Russian). (1984)

28. Raizer Yu P, Milikh G M, Shneider M N, Novakovski S. V.. Long streamers in the upper atmosphere above thundercloud. J. Phys. D: Appl. Phys. 31 3255–3264 (1998)

29. Gurevich A.V.,.Zybin K.P. Breakdown by run-out electrons during thunderstorm. Uspehi Fizicheskih Nauk. 171, No.11. 1177-1199 (in Russian) (2001)